Monte Carlo Simulation of Fatigue Crack Initiation at Elevated Temperature

Feifei He[1,*], Cher Ming Tan[1,2], Shuai Zhang[1], Shuguang Cheng[3]

[1] School of Electrical and Electronic Engineering, Nanyang Technological University, Singapore 639798
[2] SIMTech-NTU Joint Lab on Reliability, Singapore
[3] School of Materials Science and Engineering, Nanyang Technological University, Singapore 639798
* Corresponding author: ffhe@ntu.edu.sg

Abstract In this paper, a novel way that simulated the micro-crack initiation due to void nucleation under thermal fatigue was proposed using the combination of finite element modeling and Monte Carlo method. A 3D model that simulated the dynamic void nucleation process was constructed using the commercial FEA software ANSYS. The strain and thermal energies of the model due to the applied loads at elevated temperature are calculated. After manually including the grain structures, surface and bonding energies, a number of vacancies were randomly generated and they moved and nucleated according to the energy distributions of the model. To consider the problem at microscopic scale while still maintaining acceptable accuracy, two models are constructed, namely a real-sized full model and a micro-scale sub-model that included the microstructure. The impurities and the residue stresses that may affect the void nucleation process were included in the sub-model as well. The simulation results showed that the vacancies tended to nucleate at the "weak spots".

Keywords Metal fatigue, micro-crack initiation, finite element modeling

1. Introduction

Fatigue is the progressive damage to the material under cyclic loading and unloading. Cracks initiate at the stress concentration centers such as the surfaces, persistent slip bands or grain boundaries. The material eventually fractures even if the load is below its yield strength limit [1].

The initiation of the crack is due to the nucleation of tiny voids during the fatigue process [2]. Many simulation and experimental work had been conducted in the literature to study the crack initiation process using various approaches. For example, Piques *et al.* proposed a crack initiation model in 316L stainless steel based on the intergranular damage accumulation in the crack tip stress-strain field [3]. Nowack *et al.* studied the crack initiation and propagation of a Al 7475 sample under biaxial loading using the modified EVICD approach [4]. Haddar *et al.* developed a 2D model that simulated the crack initiation and shielding effects under thermal fatigue using the linear accumulation damage model [5]. Fine *et al.* predicted the fatigue crack initiation in single crystal iron and copper using the continuum models [6].

However, all the above-mentioned methods are modeled at macroscopic scale (i.e. mm scale). In fact, the voids inside the metal become visible at the size of 1 μm [7], which means the nucleation of the tiny voids start at microscopic scale. Such small crack is outside the regime of the conventional Paris's law and thus the traditional lifetime prediction cannot be applied. Furthermore, at micrometer scale, the change in lattice orientation affects the anisotropic stress distributions near the grain boundaries and this effect should not be ignored.

There is a number of reported works that studied the impact of microstructures on fatigue crack initiation. Vehoff *et al.* predicted the crack initiation at the grain boundary interfaces using the combination of the EBSD methods and the finite element stress analysis [8]. A microstructure sensitive crack nucleation criterion based on the local effective stresses and the non-local plastic strains and strain gradients was proposed by Kirane *et al.* [9]. Manonukul *et al.* developed a polycrystal plasticity finite element model that simulated the fatigue crack initiation based on the

critical resolved shear stress and the critical accumulated slip [10]. However, the dynamic void nucleation process under the applied loads was unable to be observed using the above methods.

Monte Carlo method, based on repeated random sampling algorithm [11], can be used to predict the grain size and structure [5], the crack growth and propagation [12, 13], the fatigue life and S-N curves [14, 15]. Monte Carlo method can also be used to simulate the diffusion and nucleation of the atoms under the applied loads (e.g. current, temperature, stress, etc.) [16-18]. To study the dynamic void nucleation and crack initiation process under fatigue, a novel way was introduced in this paper by incorporating the Monte Carlo method into the finite element models. Using this method, the dynamic motion of the atoms and vacancies before, during and after certain load cycle under the effects of temperature, stress, microstructure and surface condition forces and can be examined. The crack is assumed to initiate at the location of the void nucleation. Pure Al samples are used in this work.

2. Simulation Setup

The simulation is first performed on a dog-bone Al sample with the dimension shown in Figure 1. The chemical composition and the material properties measured from the sample are shown in Table 1 and 2 respectively.

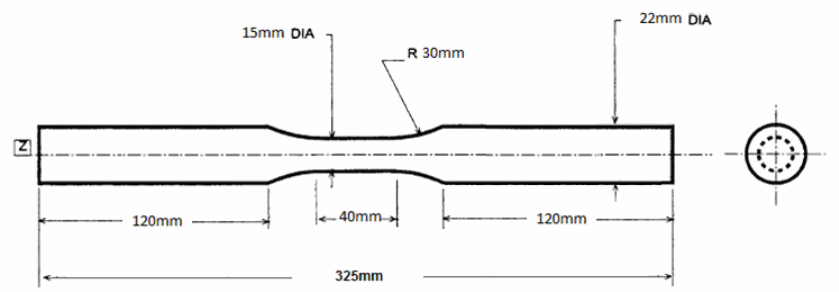

Figure 1. The dimension of the Al sample

Table 1. Chemical composition of the Al sample

ppm (parts per million)														
Al	Si	Fe	Cu	Mn	Mg	Cr	Ni	Zn	Ti	Ga	Pb	B	V	Zr
99.996%	6.20	2.20	0.10	3.90	1.00	1.20	0.30	2.70	1.10	5.50	0.10	0.80	2.40	0.80

Table 2. Physical properties of the Al sample

Young's Modulus (GPa)	Poisson's Ratio	Density (kg/m^3)	Thermal Expansion ($1/^oC$)	Yield Strength (GPa)	Thermal Conductivity ($W/m\cdot^oC$)	Specific Heat ($J/kg\cdot^oC$)
70	0.35	2700	2.24×10^{-5}	280	221.75	899.56

The initial temperature of the sample is assumed to be 27 ^oC and it is placed inside an oven with a constant temperature of 100 ^oC and heated up for 10 minutes. The convection heat transfer coefficient of the sample is 25 $W/m^2\cdot^oC$ [19]. A force of 5 kN is applied at one side of the sample and the other side is fixed and is not free to move. Finite element SOLID 69 and SOLID 45 is used in the thermal and structural-thermal simulation in ANSYS respectively.

To include the microstructure and the surface effects, a 70 μmx60 μmx30 μm sub-model is cut out from the central surface of the dog-bone sample (i.e. the full model), and the grain structures are added to the sub-model according to the EBSD map of this surface. The meshed full model and sub-model are shown in Figure 2. The nodal temperature and stress values extracted from the full model simulation are used as the boundary conditions for performing the sub-model simulation.

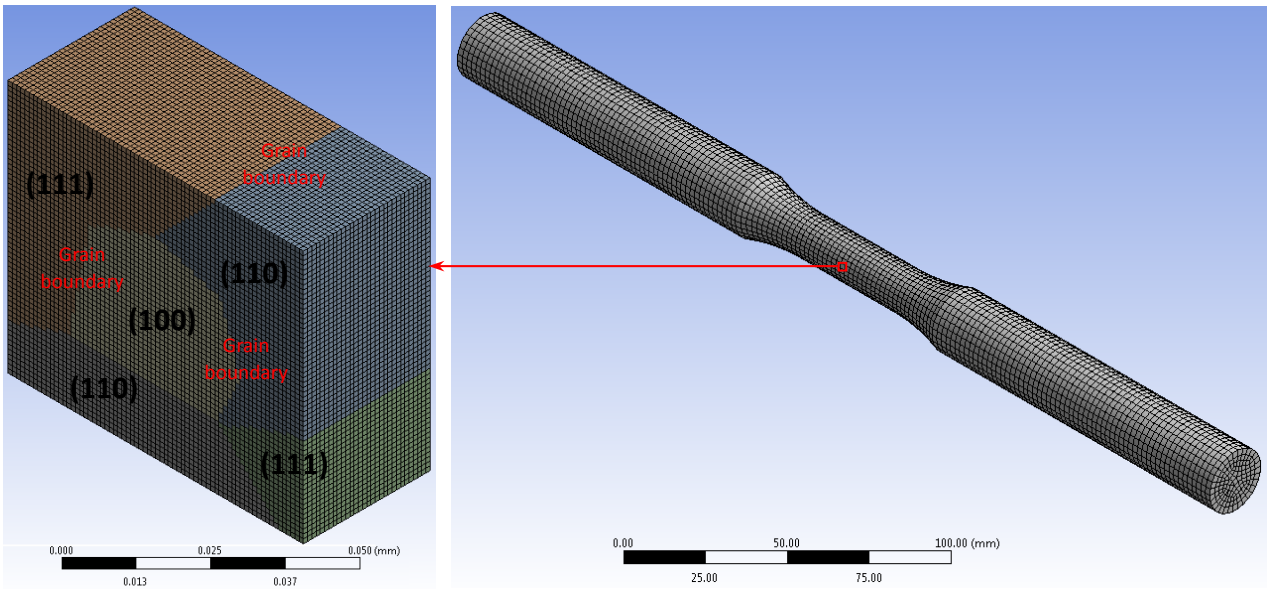

Figure 2. The micro-scale sub-model (left) cut out from the real-sized full model (right)

The nucleation of the voids is due to the movement of the atoms and the vacancies in the material, which is in turn determined by their energy states. With the presence of the external and internal factors, the atoms move and fill in the position of their neighboring vacancies in order to lower the total energy state of the system. The continuous movement causes the nucleation of the voids and the formation of the micro-cracks.

There are three types of energies that determine the total energy state of an atom, namely the thermal energy, the strain energy, and the pairing energy. The thermal and strain energy are external excitations due to the applied temperature and force respectively. The pairing energy is the energy required to excite the atom from its lowest energy state and free it out from its surrounding atoms. The pairing energy is the sum of the total bonding energy of the atom with its nearest neighbors, and is affected by the lattice orientation, the presence of the vacancies and impurities, as well as the surface condition.

The external excitations rise the energy state of the atom and when they are high enough to overcome the energy barrier (i.e. the pairing energy), the atom will become unstable and move to its neighboring vacant lattice site, as shown in Figure 3.

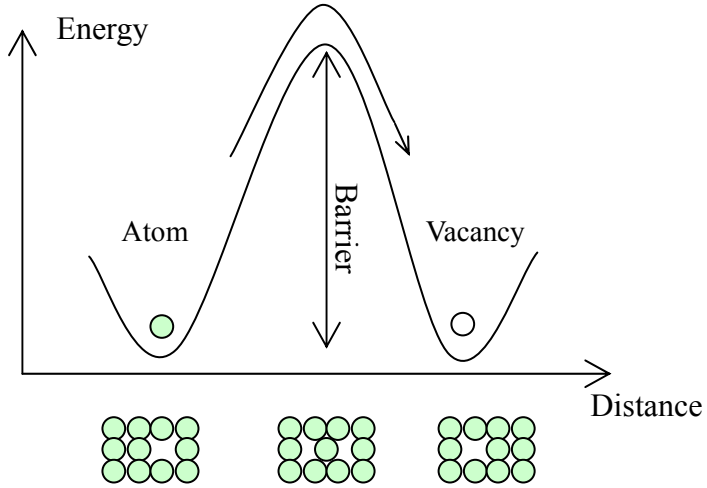

Figure 3. The movement of an atom from its original position into a vacant lattice site

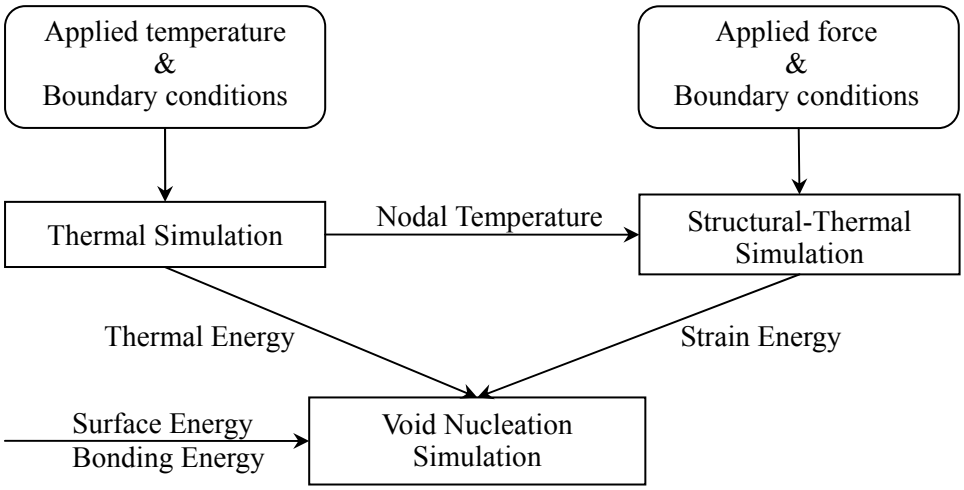

Figure 4. The flow chart of the ANSYS simulation

Figure 4 shows the flow chart of the ANSYS simulation. Based on the values computed in the thermal and structural thermal simulations, the thermal and strain energy are calculated using Equation (1) and (2) respectively [20],

$$E_{th} = N \times \frac{3}{2} k_B T \tag{1}$$

$$E_{str} = E_e^{el} + E_e^{pl} = \frac{1}{2}\{\sigma\}^T \{\varepsilon^{el}\} vol_e + \{\sigma\}^T \{\Delta\varepsilon^{pl}\} vol_e \tag{2}$$

where N is the number of the atoms, T is the location temperature, k_B is the Boltzmann's constant, E_e^{el} and E_e^{pl} are the elastic and plastic strain energy respectively, $\{\sigma\}$ is the stress vector, $\{\varepsilon^{el}\}$ is the elastic strain vector, $\{\Delta\varepsilon^{pl}\}$ is the plastic strain increment, and vol_e is the volume of the atom.

Depending on the position of the atom and the types of its neighboring atoms, the bonding energy are classified as the following categories in our simulation, as shown in Figure 5.

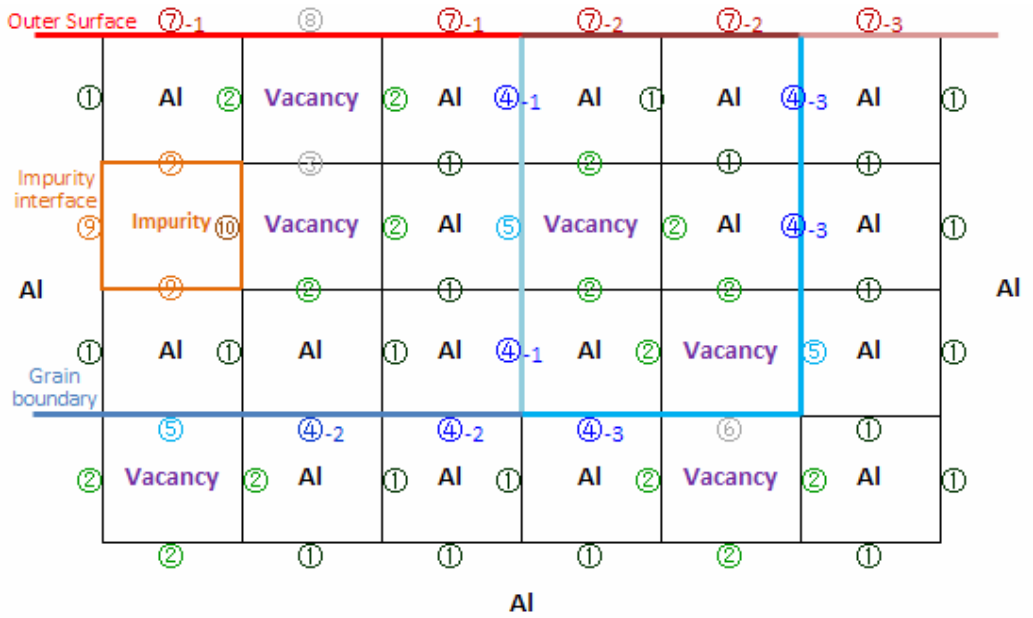

Figure 5. Different types of bonding energies used in the simulation in 2D view

(1) Inside the grain:
- Type 1: bonding energy between the Al atoms

- Type 2: bonding energy between the Al atom and the vacancy
- Type 3: bonding energy between the vacancies

(2) On the grain boundary:
- Type 4: bonding energy between the Al atoms on the grain boundary
- Type 5: bonding energy between the Al atom and the vacancy on the grain boundary
- Type 6: bonding energy between the vacancies on the grain boundary

(3) On the surface:
- Type 7: surface energy of the Al atoms with different lattice orientation
- Type 8: surface energy of the vacancies

(4) In contact with the impurity (if any):
- Type 9: adhesion energy between the Al atom and the impurity
- Type 10: bonding energy between the vacancy and the impurity

The bonding energy between the Al atoms inside the grain is 1.50 eV [21]. The bonding energy between the Al atom and the vacancy is 0.29 eV [22], and that between the vacancies is assumed to be zero. The surface energies of Al for lattice orientation (100), (110), and (111) are calculated as 0.95, 1.02 and 0.79 J/m^2 respectively using the density function theory (DFT) and the VASP software [23]. The surface energy of the vacancy is assumed to be zero. The bonding energy for the atoms on the grain boundary is approximated to be 40% of that inside the grain [24, 25]. The adhesion energy between the Al atom and the impurity (e.g. Si) is 1.09 J/m^2 [26], and 0.20 eV is used as the bonding energy between the vacancy and the Si impurity [27]. The Young's Modulus of Al for lattice orientation (100), (110), and (111) are calculated as 63.05, 71.88 and 76.05 GPa respectively [28].

The probability of atom to fill in its neighboring vacant lattice site is calculated using Equation (3) [16],

$$Probability = \exp\left(-\frac{\Delta E_{th} + \Delta E_{str} + \Delta E_{pair}}{N \times k_B T}\right) \tag{3}$$

where ΔE_{th}, ΔE_{str} and ΔE_{pair} are the change in thermal, strain and pairing energy between the target position and the original position of the atom respectively.

To begin the void nucleation simulation, 0.01% to 0.1% vacancies are randomly generated inside the sub-model depending on whether it is inside the grain or on the grain boundary [29, 30]. A few Si impurities are generated on the grain boundary as well. As the voids are only visible at micrometer scale [7], we assume the initial size of the vacancy to be 1 μm^3, which is also the size of one element in the sub-model. The thermal and strain energy of each element are calculated using Equation (1) and (2), and the pairing energy is calculated based on the position of the element and the number and type of its neighboring elements. In the Monte Carlo subroutine, a vacant site is randomly selected and total change in energy between the selected vacancy and its neighboring elements are computed. The neighboring element exchange position with the vacancy (i.e. fill in the position of the vacant site) if the probability of movement is larger than 0.5 [25]. The continuous position swapping process results in the movement of the vacancies and the nucleation of the voids.

3. Results and discussions

The position of the vacancies at the beginning, during and the end of the simulation after 1500 Monte Carlo cycles are shown in Figure 6(a) (b), and (c) respectively.

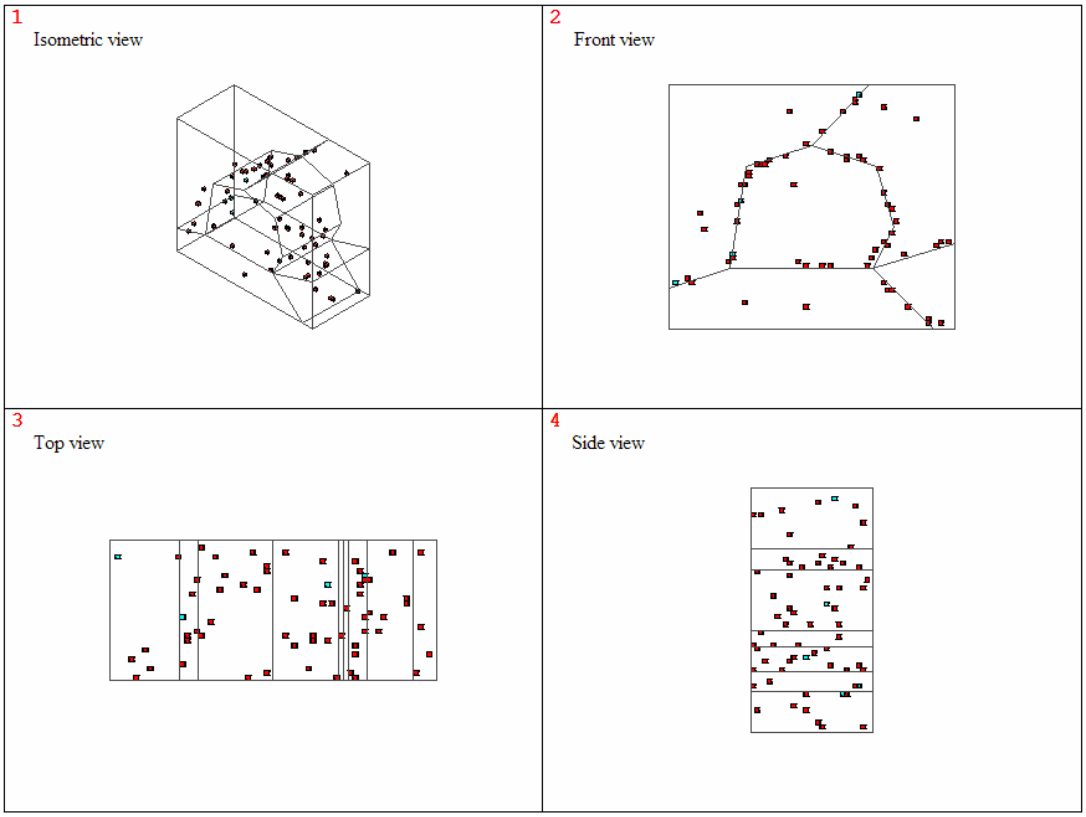
1
Isometric view
2
Front view
3
Top view
4
Side view

(a)

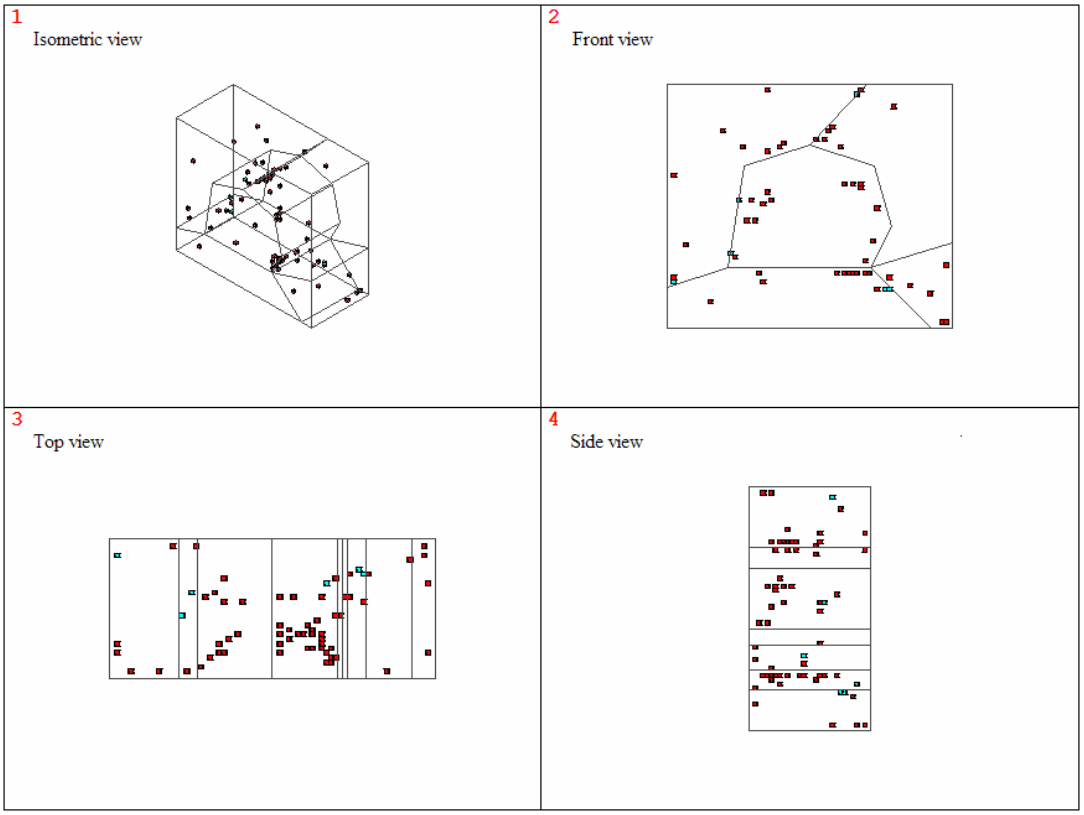
1
Isometric view
2
Front view
3
Top view
4
Side view

(b)

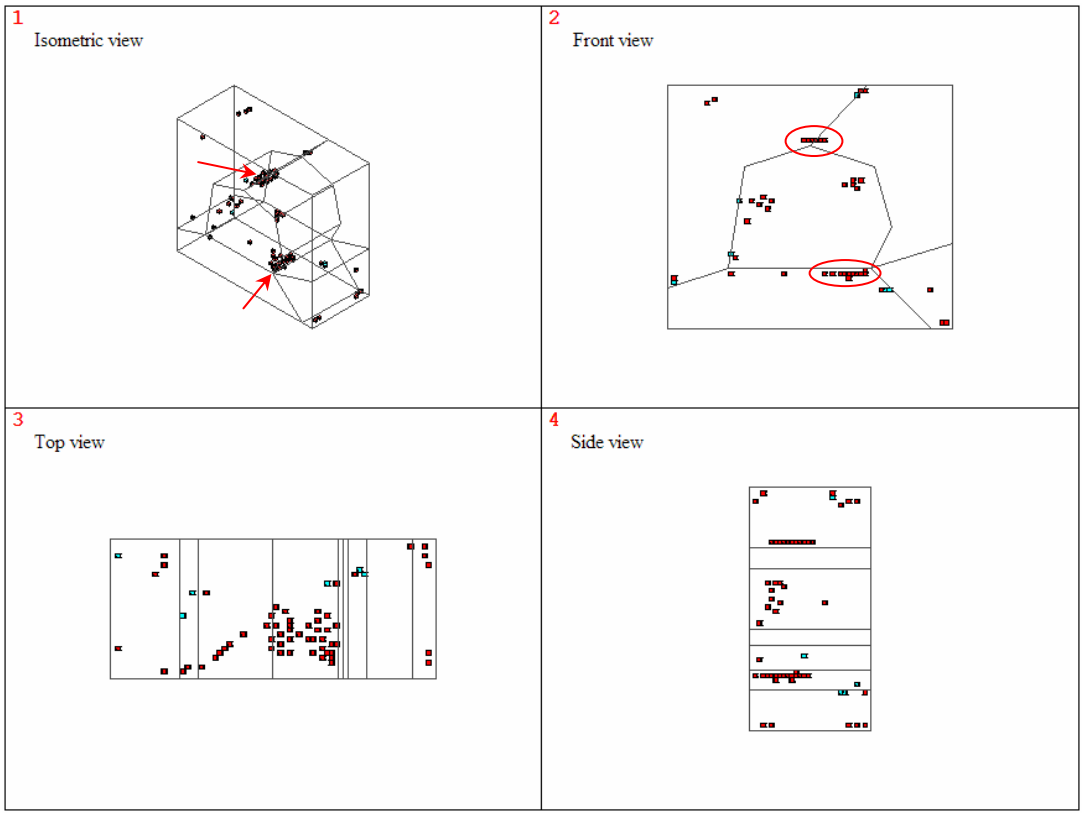

(c)

Figure 6. The vacancy position (a) at the beginning (b) during and (c) at the end of the simulation. The red dots are the vacancies and the blue dots are the impurities.

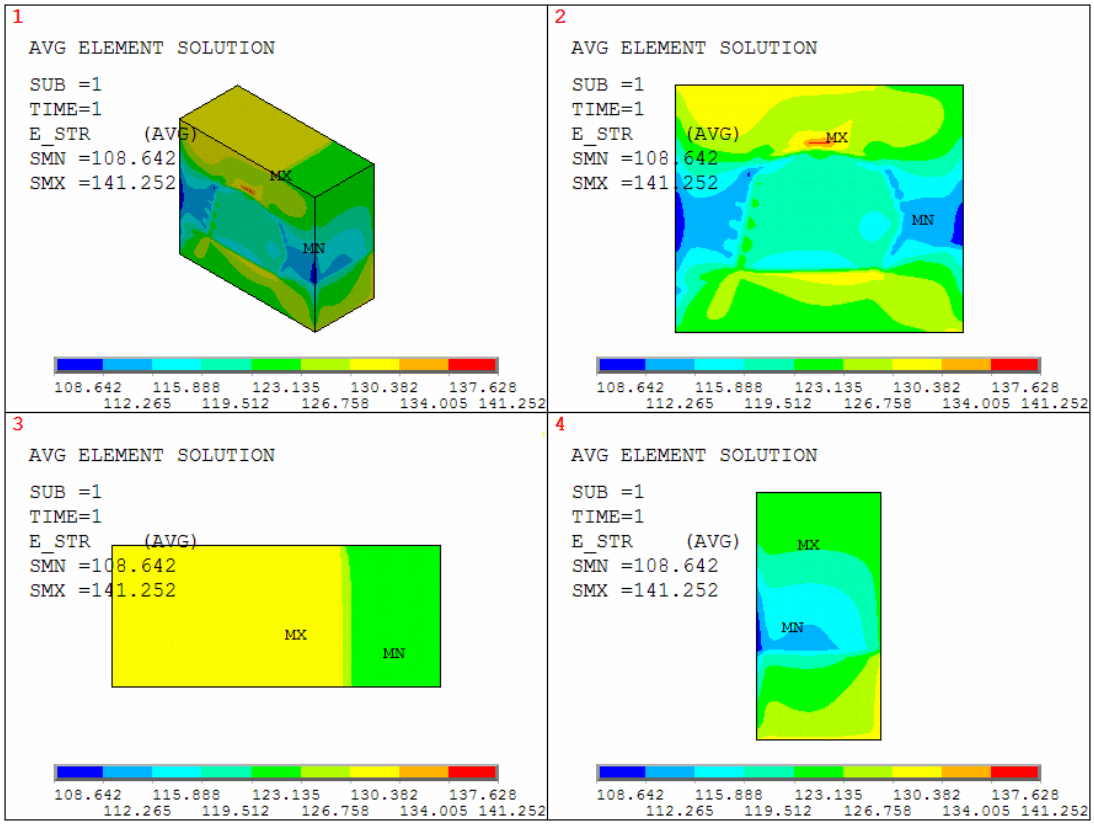

Figure 7. The strain energy distribution of the sub-model. High strain energy concentration is found at grain boundary triple point region.

From Figure 6, it can be seen that most of the vacancies nucleate at the grain boundary triple point region, as shown by the arrows and circles. This is because the stress inhomogeneity between different grains causes the concentration in strain energy along the grain boundary, especially at the triple point, as can be seen in Figure 7. Hence the vacancies tend to move to these regions in order to lower the total energy of the system. On the other hand, the presence of the impurities increases the stress around them slightly. This causes a slight instability in energy in the regions around the impurities. Therefore the impurities are able to attract some of the vacancies as well, and a few red spots are found around the blue spots in Figure 6.

The presence of the residue stress may increase or decrease the stress state on the sub-surface depending on whether it is tensile or compressive. This can affect the void nucleation process as well. The simulation is performed again with 10% increase in sub-surface stress due to tensile residue stress and the final vacancy position is shown in Figure 8. It can be seen that the presence of the residue stress attracts some vacancies to the surface, as shown by the arrows and the rectangle in Figure 8. Additional cracks may form at this region.

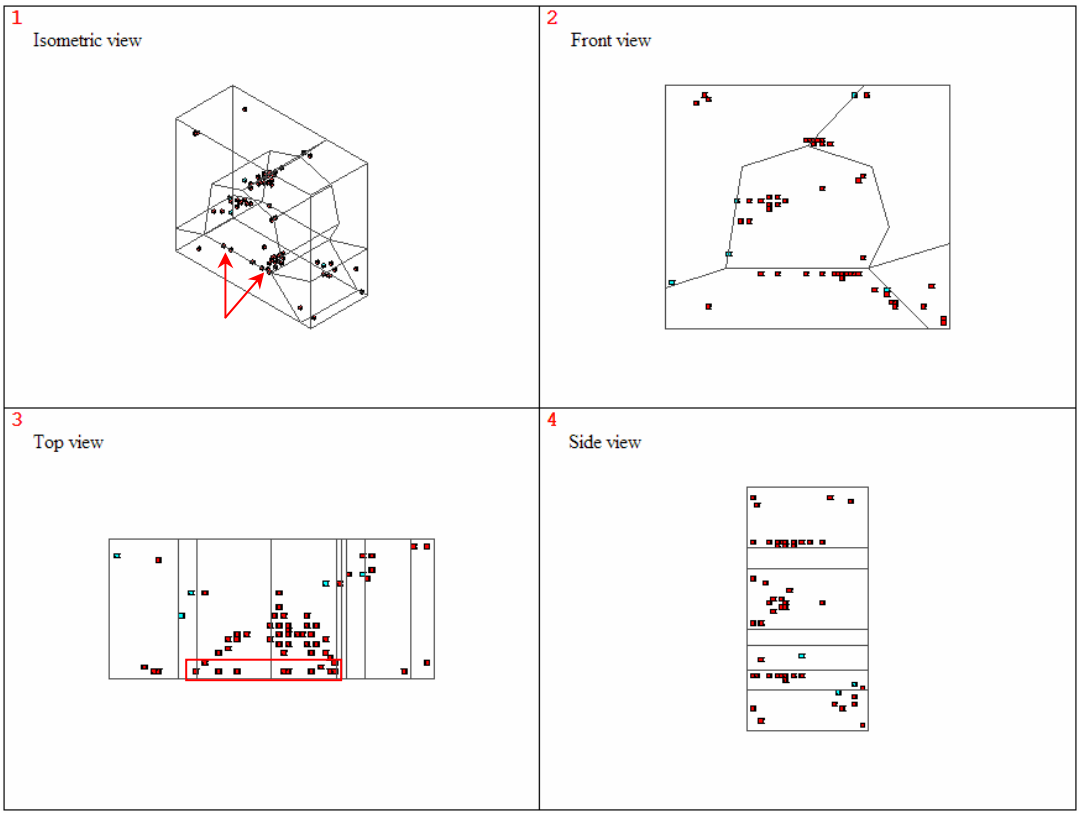

Figure 8. The vacancy position at the end of the simulation with the presence of the residue stress.

4. Conclusions

A finite element model that simulated the void nucleation process under thermal fatigue using the combination of finite element modeling and Monte Carlo method was presented in this paper. The simulation was first performed on a real-sized full model that contained the real time temperature and stress profile of the sample. The simulation was then carried out on a micro-scale sub-model that contained the microstructure and the imperfections, as well as different bonding and surface energies caused by the change in lattice orientation. The movement of the vacancies due to the uneven energy distributions of the model was observed and the void nucleated at the region with higher strain energies (i.e. the “weak spot”). Experimental verification of our method is underway.

References

[1] W.H. Kim, C. Laird, Crack nucleation and state I propagation in high strain fatigue-II mechanism. Acta Metallurgica, (1978) 789-799.
[2] R.L. Lyles, H.G. F. Wilsdorf, Microcrack nucleation and fracture in silver crystals. Acta metall, 23 (1975), 269-277.
[3] R. Piques, P. Bensussan, A. Pineau, Crack initiation and growth under creep and fatigue loading of an austenitic stainless steel. Nuclear Eng and Design, 116 (1989) 293-306.
[4] H. Nowack, D. Hanschmann, W. Ott, K.-H. Trautmann, E. Maldfeld, Crack initiation life behavior under biaxial loading conditions-experimental behavior and prediction. SAE Special Publications, 1280 (1997) 159-183.
[5] N. Haddar, A. Fissolo, 2D simulation of the initiation and propagation of crack array under thermal fatigue. Nuclear Eng and Design, 235 (2005) 945-964.
[6] M.E. Fine, P. Bhat, A model of fatigue crack nucleation in single crystal iron and copper. Mater Sci Eng A, 468-470 (2007) 64-69.
[7] J. Belak, On the nucleation and growth of voids at high strain-rates. J Computer-Aided Materials Design, 5 (1998) 193-206.
[8] H. Vehoff, A. Nykyforchyn, R. Metz, Fatigue crack nucleation at interfaces. Mat Sci Eng A, 387-389 (2004) 546-551.
[9] K. Kirane, S. Ghosh, M. Groeber, A. Bhattacharjee, Grain level dwell fatigue crack nucleation model for Ti alloys using crystal plasticity finite element analysis. J Eng Mat Tech, 131 (2009) 021003.
[10] A. Manonukul, F.P.E. Dunne, High- and low-cycle fatigue crack initiation using polycrystal plasticity. in: Proc Royal Society of London, Series A (Mathematical, Physical and Engineering Sciences), 2004, vol. 460, no. 2047, pp. 1881-903.
[11] K. Binder, D.W. Heermann, Monte Carlo Simulation in Statistical Physics: An Introduction, 4th ed, Springer, Berlin, 2002.
[12] B.N. Cox, W.L. Morris, Monte Carlo simulations of the growth of small fatigue cracks. Eng Fracture Mechanics, 31 (1988) 591-610.
[13] T. Shimokawa, Y. Kakuta, Application of Monte Carlo simulation for fractographic analysis of fatigue crack propagation, Inter J Fatigue, 18 (1996) 321-327.
[14] Y. Zhao, Monte Carlo simulation and modification on the historic probabilistic fatigue S-N curves. in: Proc IEEE 10th Inter Conf on Computer-Aided Industrial Design & Conceptual Design, 2009, pp. 2323-2327.
[15] C.M. Kim, J.K. Kim, C.S. Kim, Fatigue life evaluation of ERW joint in the pipe using Monte-Carlo simulation. Key Eng Mat, 297-300 (2005) 3-9.
[16] T.J. Smy, S.S. Winterton, M.J. Brett, A monte carlo computer simulation of electromigration. J App Phy, 73 (1993) 2821.
[17] P. Bruschi, A. Nannini, M. Piotto, Three-dimensional Monte Carlo simulations of electromigration in polycrystalline thin films. Computational Material science, 17 (2000) 299-304.
[18] W. Li, C.M. Tan, Dynamic simulation of electromigration in polycrystalline interconnect thin film using combined Monte Carlo algorithm and finite element modeling, in: Symp Microelectronics, Singapore, 2006.
[19] http://www.engineeringtoolbox.com/overall-heat-transfer-coefficient-d_434.html
[20] ANSYS, Theory Reference and reference therein
[21] D.R. Askeland, The Science and Engineering of Materials, PWS-Kent Publishing Co., 1987.
[22] J.E Epperson, P Fürnrohr, V. Gerold, Two stages of binding energy between vacancies and in atoms in an Al matrix. Mat Sci and Eng, 19 (1975) 95-103.
[23] X.-G. Wang, A. Chaka, M. Scheffler, Effect of the environment on α-Al_2O_3 (0001) surface structures. Phsical Review Letters, 84 (2000) 3650-3653.

[24] T.V. Zaporozhets, A.M. Gusak, K.N. Tu, S.G. Mhaisalka, Three-dimensional simulation of void migration at the interface between thin metallic film and dielectric under electromigration. Appl Phys Letter, 98 (2005) 103508.

[25] R.R. Atkinson. Ph.D New Brunswick Rutgers, The State University of New Jersey, 2003.

[26] P. Shen, H. Fujii, K. Nogi, Wetting, Adhesion and Adsorption in Al-Si/(0112) α-Alumina System at 1723K. Materials Transactions, 45 (2004) 2857-2863.

[27] J. Burke, A determination of the binding free energy between vacancies and silicon solute atoms in aluminium using an equilibrium method. Philosophical Magazine, 21 (1970) 7-22.

[28] S. Zhang, S. Cheng, H. Su, C.M. Tan, F. He, ab-initio computation of some surface and material properties of Aluminum and Silicon, in preparation for submission to IEEE Trans. On Nanotechnology.

[29] B.V. Guerard, H. Peisl, R. Zitzmann, Equilibrium vacancy concentration measurements on aluminum. Applied Physics B, 3 (1974) 37.

[30] K.M. Carling, G. Wahnstrom, T.R. Mattsson, N. Sandberg, G. Grimvall, Vacancy concentration in Al from combined first-principles and model potential calculations. Phys Review B, 67 (2003) 054101.